Fourth International Symposium on Marine Propulsors
smp'15, Austin, Texas, USA, June 2015

Influence of the Turbulence Closures for the Wake Prediction of a Marine Propeller

E. Guilmineau, G.B. Deng, A. Leroyer, P. Queutey, M. Visonneau, J. Wackers

LHEEA, CNRS UMR 6598, Ecole Centrale de Nantes
BP 92101, 44321 Nantes Cedex 3, France

ABSTRACT

Results of computational fluid dynamics validation for flow around a marine propeller are presented. Computations were performed for various advance coefficients following experimental conditions. The objectives of this study are to establish capabilities of various turbulent closures to predict the wake of a propeller, and to predict the instability processes in the wake. Two RANS models are used: the k-ω SST of Menter and an anisotropic two-equation Explicit Algebraic Reynolds Stress Model (EARSM). A DES approach based on the k-ω model is also used. Computational results for both global and local flow quantities are discussed and compared with experimental data. The predicted thrust and torque are in good agreement with the measured values for all turbulent closures. With the RANS turbulence models, the wake of the propeller is too dissipated and then the instabilities of the wake are not predicted. On the contrary, DES approach can allow to capture the evolution of the tip vortices and predicts the onset of instabilities in the wake. The main difference between these various turbulence closures is that the flow in the core of the vortex is characterized by rotation, streamline curvature effects which are not adequately modelled by RANS turbulence models.

Keywords

Propeller, Open water, Numerical simulations, Turbulence models, DES approach, RANS models.

1 INTRODUCTION

The prediction of the fluid dynamics interaction between propellers and the hull is very important for the improvement of ship performance since the interaction is directly related to vibrations, noise and propulsion performances. In this context, the demand for the improvement of performance implies a rising interest in the development and application of detailed numerical tools

The physical mechanisms that characterize the interaction between the propeller and the hull are very complex. However, even in the simpler case of an isolated propeller in a uniform flow, called open water conditions, we are confronted with several numerical and physical challenges. In the propeller field, a number of viscous phenomena can be identified including blade and hub boundary layers, flow separation on the blade, viscous-inviscid interaction, hub and tip vortices, viscous wake. Therefore, study of these flow characteristics is essential for accurate prediction of the propulsion performance. In this paper, we only focus on the open water conditions. In this case, the flow is characterized by two vortex systems: one generated by the tip of the blade and the second emanated from the hub. A comprehensive description of the state of the art can be found in Felli et al. (2011), who experimentally investigated the flow around a propeller in water tunnel. These authors studied the mechanisms that trigger the instability of wake and investigated the dependence of the vortex pairing and grouping on the mutual vortex distance.

Based on a numerical point of view, the reliability of the such numerical predictions can be questioned. It is difficult to control numerical diffusion when intense and localized three-dimensional structures are concerned. The flow in the core of the vortex is characterized by rotation, streamline curvature effects which are not adequately modeled by classical eddy-viscosity based turbulence models. Unsteady hybrid LES turbulence closures like DES appear attractive, see Muscari et al. (2013).

The purpose of this paper is to conduct such a validation of the flow around an isolated propeller to compare statistical turbulence closures and an hybrid LES methodology to draw conclusions about the requirements in term of physics. The present paper is organized as follows. The test-case is presented followed by the numerical method. The CFD results are presented for comparison and validation, as well as flow field analysis. Lastly, some concluding remarks are made.

2 TEST-CASE

The propeller geometry is the INSEAN E779A model, i.e. a four bladed, fixed-pitch, right-handed propeller

characterized by a nominally constant pitch distribution and a very low skew angle. The propeller is presented in Figures 1 and 2 and the main geometrical features are reported in Table 1.

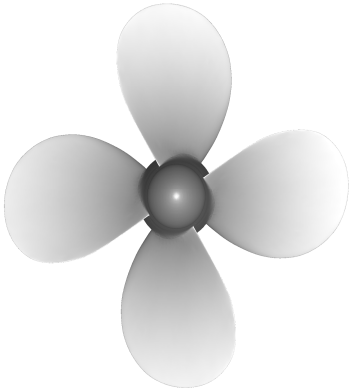

Figure 1: Front view of the propeller model.

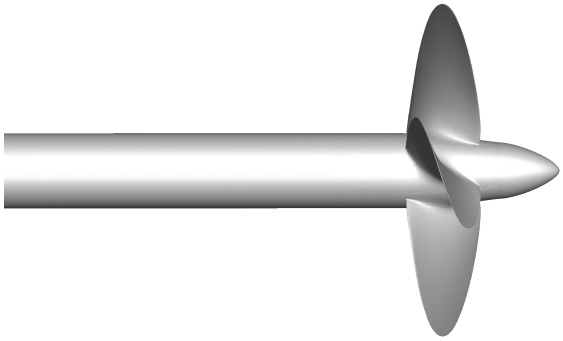

Figure 2: Side view of the propeller model.

Table 1: Propeller parameters of INSEAN E779A model.

Diameter	D = 0.227 m
Number of blades	Z = 4
Pitch ratio	P/D = 1.1
Rake	4°35' (forward)
Expanded area ratio	0.689
Hub ratio	0.200

In this paper, the rotational speed of the propeller is kept fixed to a value of n = 25 rps and the different advance coefficients $J = U_\infty/(nD)$ are obtained by changing the inflow velocity U_∞. The Reynolds number $Re = 1.78\times10^6$ is based on the radius of the propeller (L_{ref} = R = 0.1135 m) and the velocity of the tips of the blades ($U_{ref} = n\pi D \approx$ 17.829 m/s)

3 ISIS-CFD AT GLANCE

The solver ISIS-CFD, available as a part of the FINE^{TM}/Marine computing suite, is an incompressible unsteady Reynolds-averaged Navier-Stokes (URANS) method mainly devoted to marine hydrodynamics. The method features several sophisticated turbulence models: apart from the classical two-equation k-ε and k-ω models, the anisotropic two-equation Explicit Algebraic Reynolds Stress Model (EARSM), as well as Reynolds Stress Transport Models (RSM), are available, see Deng & Visonneau (1999) and Duvigneau et al. (2003), with or without rotation corrections. All models are available with wall-function or low-Reynolds near wall formulation. Hybrid LES turbulence models based on Detached Eddy Simulation (DES) are also implemented and have been validated on automotive flows characterized by large separations, see Guilmineau et al. (2011). Additionally, several cavitation models are available in the solver.

The solver is based on the finite volume method to build the spatial discretization of the transport equations. The unstructured discretization is face-based. While all unknown state variables are cell-centered, the system of equations used in the implicit time stepping procedure are constructed face by face and the contribution of each face is then added to the two cells next to the face. This technique poses no specific requirements on the topology of the cells. Therefore, the grids can be completely unstructured: cells with an arbitrary number of arbitrarily-shaped faces are accepted. Pressure-velocity coupling is enforced through a Rhie & Chow SIMPLE type method: at each time step, the velocity updates come from the momentum equations and the pressure is given by the mass conservation law, transformed into a pressure equation. In the case of turbulent flows, transport equations for the variables in the turbulence model are added to the discretization

Free-surface flow is simulated with a multi-phase flow approach: the water surface is captured with a conservation equation for the volume fraction of water, discretized with specific compressive discretization schemes, see Queutey & Visonneau (2007). The technique included for the 6 degrees of freedom simulation of ship motion is described by Leroyer & Visonneau (2005). Time integration of Newton's law for the ship motion is combined with analytical weighted analogy grid deformation to adapt the fluid mesh to the moving ship. To enable relative motions of appendages, propellers or bodies without having recourse to overlapping grids, a sliding grid approach has been implemented. Propellers can be modeled by actuator disc theory, by coupling with boundary element codes (RANS BEM coupling, see Deng et al. (2013)) or with direct discretization through e.g. the rotating frame method or sliding interface approaches

Finally, an anisotropic automatic grid refinement procedure has been developed which is controlled by various flow-related criteria, see Wackers et al. (2014). Parallelization is

based on domain decomposition. The grid is divided into different partitions, which contain the cells. The interface faces on the boundaries between the partitions are shared between the partitions; information on these faces is exchanged with MPI (Message Passing Interface) protocol. The method works with the sliding grid approach and the different sub-domains can be distributed arbitrarily over the processors without any loss of generality. Moreover, the automatic grid refinement procedure is fully parallelized with a dynamic load balancing working transparently with or without sliding grids

4 NUMERICAL SIMULATION SET-UP

The computational domain consists of a cylindrical domain, whose diameter is 3 times the propeller diameter, and length is 9.18 times the propeller diameter. It starts 3.96R before the propeller plane and it extends until 15.4R after the propeller plane. The computational domain with the boundary conditions is presented in Figure 3.

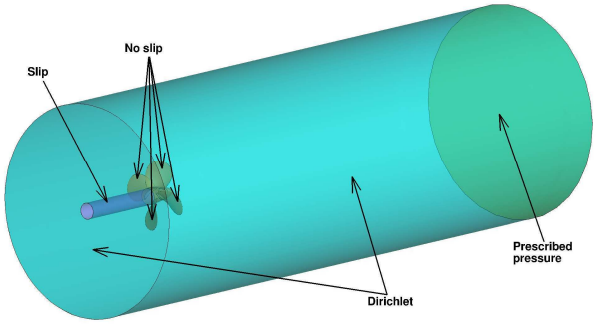

Figure 3: Computational domain with the boundary conditions.

The computational mesh is created with HEXPRESS, an automatic unstructured mesh generator. This software generates meshes containing only hexahedrons. The mesh consists of 21.4×10^6 cells. The number of faces for each blade is approximately 38,100. The average wall normal resolution on the blades is $y^+ = 0.6$ with a maximum around the tip, in the order of 1.8. A box including the propeller and extending up to 6 diameters in the wake is added to capture the vortices. In this box, the cells are isotropic and the size is 0.0105R, see Figures 4 and 5

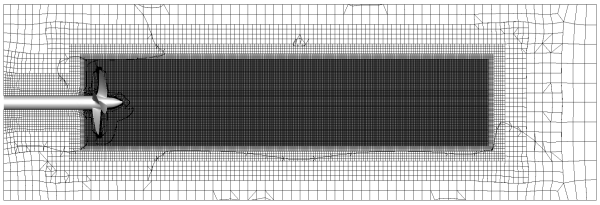

Figure 4: View of the mesh in the symmetry plane

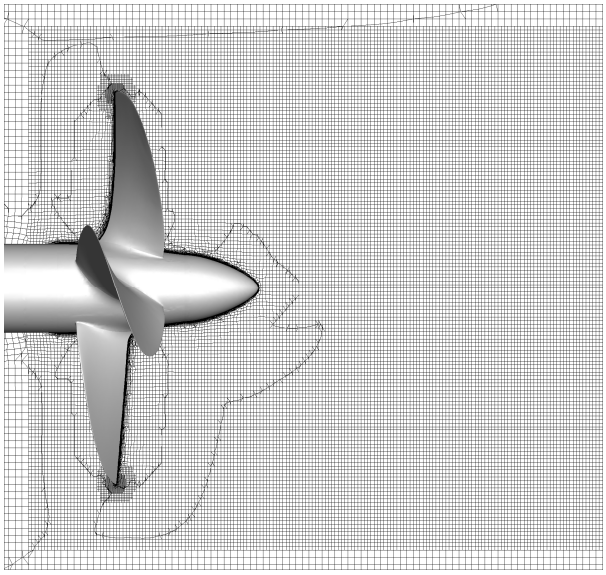

Figure 5: View of the mesh detail in the symmetry plane.

The RANS equations are written in the moving reference frame but written in terms of absolute reference quantities. For the RANS turbulence models (k-ω SST and EARSM), the solution is a steady solution while for DES computations, this approach is unsteady and the time step is 3×10^{-5} seconds. This time step corresponds to a rotation of 0.27 degrees. The time-averaged flow is obtained in approximately 9 flow-times for DES computations.

The numerical simulation is distributed on 96 processors on a SGI Altix ICE 8200. For the RANS simulations, the CPU time per processor is 23 hours while for the DES approach, it is 300 hours

5 RESULTS AND DISCUSSION

5.1 Open-water characteristics

In order to compare different turbulence models for the prediction of the flow around the propeller, the open water characteristics of the model are investigated. Several numerical results for different values of the advance coefficient J are compared with the experimental data, see Figure 6. Concerning the thrust coefficient $Kt = T/(\rho n^2 D^4)$, where T is the thrust of the propeller and ρ the density of the water, and the torque coefficient $Kq = Q/(\rho n^2 D^5)$, where Q is the torque, the predictions obtained with the different turbulence models differ by less than 5% for the low values of the advance coefficient and by less than 3% for the high value of J. The numerical propeller open-water efficiency $\eta = Kt/Kq \times J/(2\pi)$ is also in good agreement with the experimental data. From the point of view of global estimations, it therefore appears that the use of a more accurate turbulence model is not justified

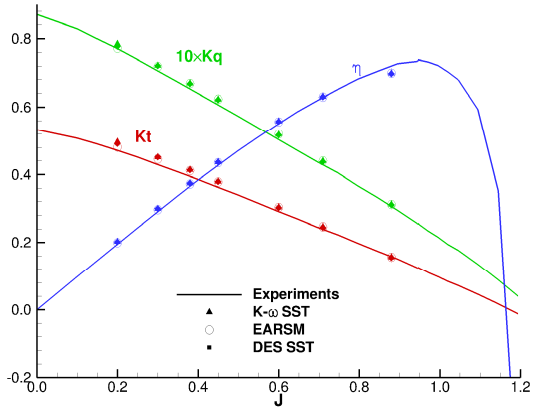

Figure 6: Open-water characteristics of the E779A propeller.

5.2 Flow field in the wake

However, it is crucial to evaluate the ability of the turbulence model to reproduce some of the findings of Felli et al. (2011). The analysis of the flow field is carried out for three values of the advance coefficient, J = 0.71, 0.45 and 0.20. All results obtained with a RANS turbulence model are steady results while for the DES results, if not explicitly mentioned, the results are issued from an averaged flow.

5.2.1 J = 0.71

A general view of the wake of the propeller, for the advance coefficient J = 0.71, is given in Figure 7 which presents an isosurface of the dimensionless value $\lambda_2 = -2$ of the second largest invariant of $\mathbf{S}^2+\Omega^2$ ($\mathbf{S}$ and Ω being the symmetric and antisymmetric component of $\nabla\mathbf{u}$) colored by the helicity. The acceleration of the flow behind the propeller causes a slight reduction of the radial position of the vortex cores. Then, the helices formed by the tip vortices remain located on a circular cylinder. RANS model yield tip vortices but they vanish more or less rapidly in the wake depending on the turbulence model used and the level of anisotropy associated with the turbulence model. With the DES approach, the tip vortices are maintained much further in the wake. These remarks are also observed by Muscari et al. (2013).

In order to have a qualitative idea of the level of mesh resolution, a view of the DES function is presented in Figure 8. The blue area corresponds to $F_{DES} \leq 1$, which represents the RANS area, while $F_{DES} > 1$ for the LES area, the red region in the figure. the resolution of propeller wake is suited to a LES approach

Figure 9 presents a comparison of the turbulence kinetic energy (TKE) and the y-component of the vorticity for the three turbulence models used. the RANS simulations, Figure 9(a) and 9(b), predict a small value of the TKE near the tip of the blade which grows rapidly in the vortex core. The values around the vortex core increase along the filament. On the contrary, the DES approach produces a high TKE near the tip but the level vanishes quickly and the level is lower than those observed with a RANS approach. Then, the level of vorticity, which is similar for all numerical simulations close to the propeller, decreases very quickly for the RANS simulations whereas for the DES the decay is more progressive

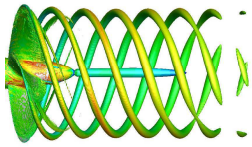

(a) k-ω SST

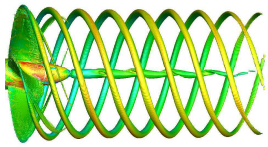

(b) EARSM

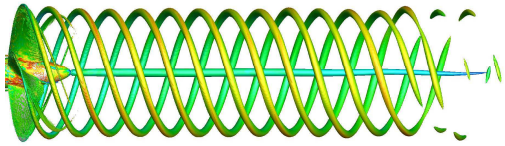

(c) DES

Figure 7: J = 0.71 - Vortical structures visualisations (λ_2 = - 2).

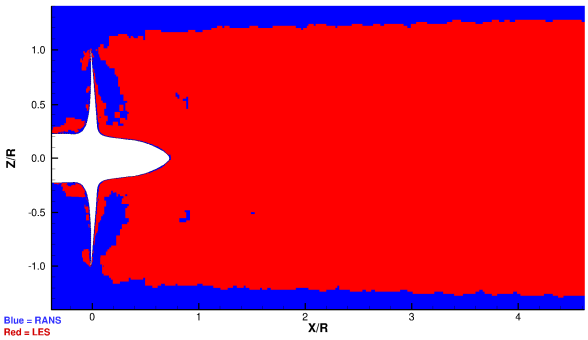

Figure 8: J = 0.71 - Visualisation of the DES function (red: LES region, blue: RANS region).

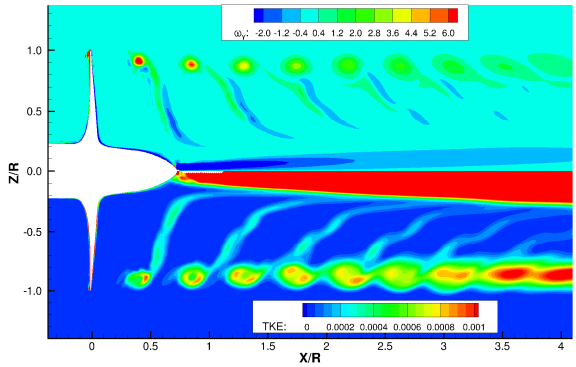

(a) k-ω SST

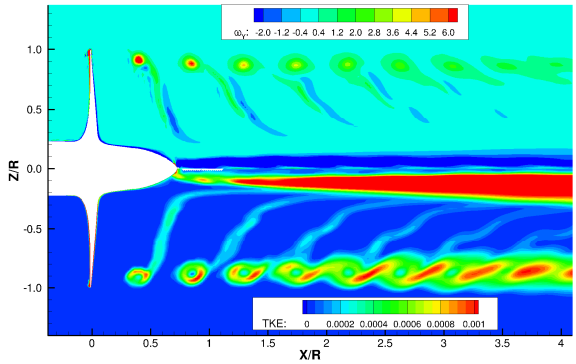

(b) EARSM

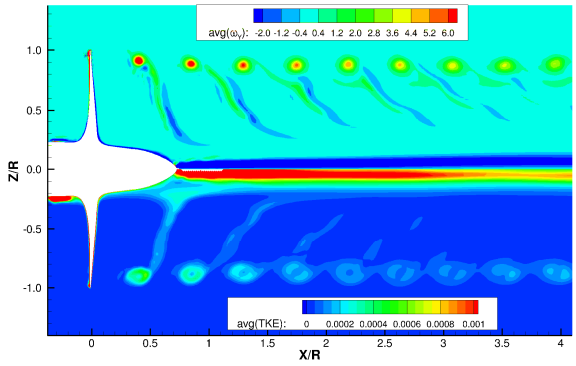

(c) DES

Figure 9: J = 0.71 - Y-component of vorticity (upper half) and turbulence kinetic energy (lower half).

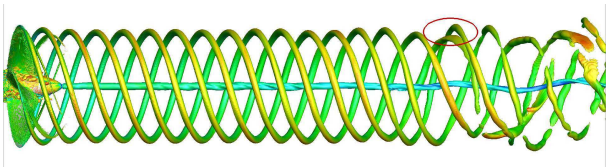

Figure 10: J = 0.71 - Instantaneous visualization of the vortical structures (λ_2 = -2).

The detailed frequency analysis performed in the experimental work illustrates the process of energy transfer from the blade harmonic to the shaft at nearly at x =7R, owing to vortex grouping. In the numerical simulation with the DES approach, the vortex grouping, marked by red ellipse, appears nearly 7.2R.

5.2.2 J = 0.45

The figure 11 presents an instantaneous view of the vortical structure obtained with the DES approach and the visualization in Felli et al. (2011). These figures are very similar and present the pairing of the vortices due to the instability of the tip vortices and the beginning of the instability of the hub vortex. The tip vortices deform from the helical path and trend to interact mutually and form a group. Then, the hub vortex undergoes a sudden deformation from a straight to a spiraling geometry. The difference between the numerical result and the experimental visualization is the spiral-to-spiral distance. In the numerical simulation, this distance is shorter than that observed in experiments. However, the numerical spiral-to-spiral distance is in agreement with the numerical simulations of Musca ri et al. (2013).

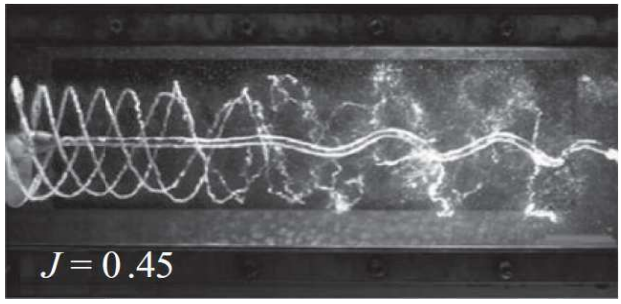

(a) Experimental view (Fig. 8 in Felli at al. (2011))

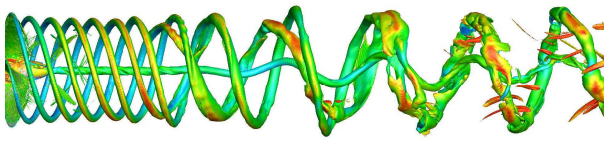

(b) Numerical results

Figure 11: J = 0.45 - Instantaneous visualization of the vortical structures.

To compare all turbulence models, the averaged flow for the DES approach is presented with the RANS results in Figure 12. For the RANS results, the characteristics of the flow are the faster deformation of the wake and the stronger tip vortices. Even if the tip vortices are stronger than those predicted with the previous advance coefficient, they are resolved over a shorter distance. This trend is also confirmed by the numerical results of Muscari et al. (2013). The DES model permits to predict more extended vortices and shows both the onset of the vortex instability and the start of the pairing process.

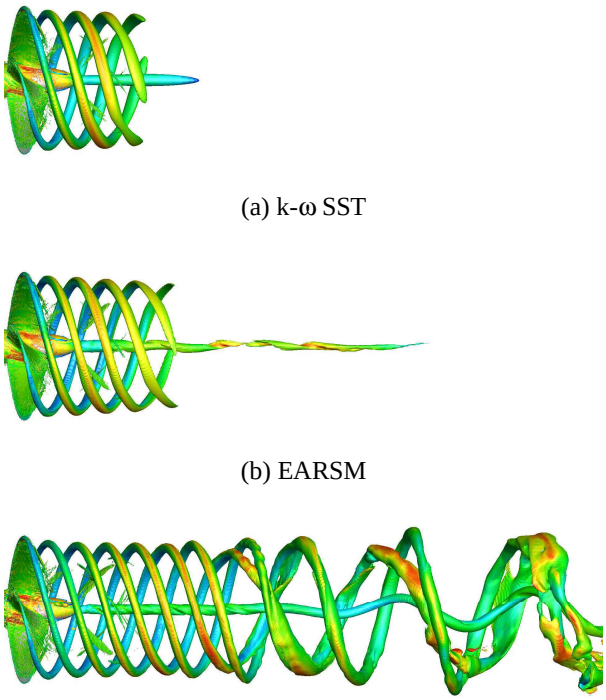

(a) k-ω SST

(b) EARSM

(c) DES

Figure 12: J = 0.45 - Vortical structures visualisations (λ_2 = -2).

A comparison of the resolved TKE and the modelled TKE is presented in Figure 13. The intensity of the resolved TKE increases, in particular in the wake where the instability process begins and the start of the pairing process between the tip vortices is clearly revealed. The modelled TKE is limited to lower levels

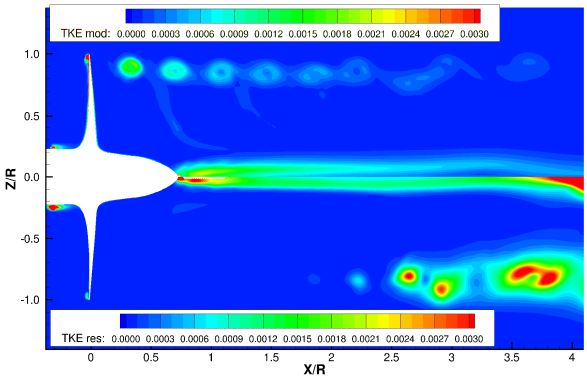

Figure 13: J = 0..45 - Modelled turbulence kinetic energy (upper half) and resolved turbulence kinetic energy (lower half).

5.2.3 J = 0.20

The last value of the advance coefficient is J = 0.20 which corresponds to a condition of very high blade loading. The wake evolution of the tip vortices decreases quickly, even for the DES approach, see Figure 14.

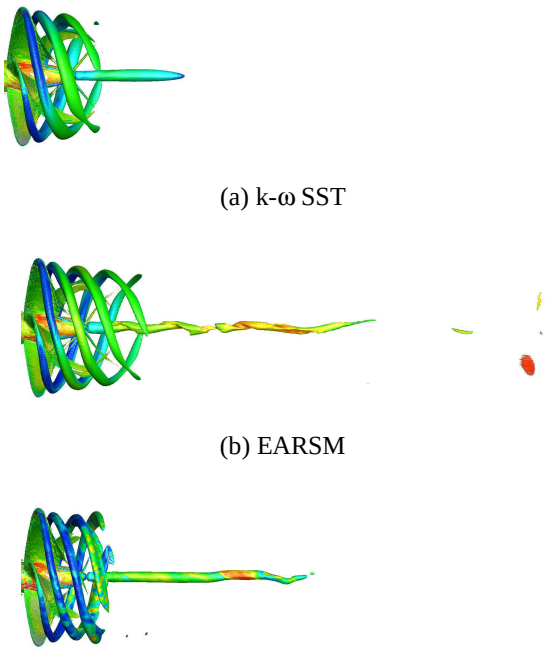

(a) k-ω SST

(b) EARSM

(c) DES

Figure 14: J = 0.20 - Vortical structures visualisations (λ_2 = -2).

Figure 15 represents a view of the instantaneous isosurface of the invariant λ_2 obtained with a DES approach. We can compare this figure with Figure 14(a) or 14(b) which represent a view with the RANS model. With the DES

approach, more structures are predicted. Even if a RANS simulation yields a good prediction of forces and moments, this approach fails to give information about the wake evolution which may be important, like for the prediction of noise or if a body like another propeller or a rudder is in its wake.

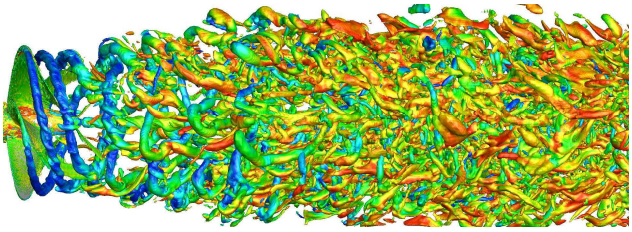

Figure 14: J = 0.20 - Instantaneous vortical structures visualization (λ_2 = -2).

4 CONCLUSIONS AND FUTURE WORK

The capabilities of numerical simulations with various turbulence closures (RANS and DES), using ISIS-CFD flow solver, to predict the complex flow past an isolated propeller have been presented in this paper. A marine propeller called INSEAN E779A was selected for the present study. Computations were performed for various advance coefficients following experimental conditions.

Computational results are discussed and compared with experimental data. The predicted global quantities, such as thrust and torque, obtained with various turbulence closures, are in good agreement with the measured data. For the prediction of the wake, a comparison between the RANS models and the DES approach shows that the RANS approach dissipates the tip vortices very quickly due to the high level of the turbulence kinetic energy in the core of the vortices. On the contrary, the DES approach allows to capture the evolution of the tip vortices. The initial stages of the instability pattern, with two consecutive filaments grouping their relative position, can also be reproduced and agree reasonably well with the flow visualization. The hybrid LES model performs better than the eddy-viscosity based turbulence closures since it is able to predict the relaminarization of the core of the tip vortex in the wake of the propeller.

The overall results suggest that the RANS approach is sufficient to predict the thrust and the torque. But if the prediction of the propeller wake is necessary, a DES approach should be used. Nevertheless, the cost of this approach is still prohibitive to be used as a matter of routine architecture design offices. However, for the propeller design to predict the cavitation risk, the DES approach has still to demonstrate its ability in predicting a better tracking of the ventilated tip vortex father downstream.

ACKNOWLEDGMENTS

This work was granted access to the HPC resources of CINES/IDRIS under the allocation 2014-2a0129 made by GENCI.

REFERENCES

Deng, G.B., Queutey, P., Visonneau, M. and Salvatore, F. (2013),), “Ship Propulsion Prediction with a Coupled RANS-BEM Approach”, Proc. of V International Conference on Computational Methods in Marine Engineering, MARINE-2013, Hamburg, Germany.

Deng, G.B and Visonneau, M. (1999), “Comparison of Explicit Algebraic Stress Models and Second-Order Turbulence Closures for Steady Flow around Ships”, Proc. of 7th Symposium on Numerical Ship Hydrodynamics, Nantes, France, 4.4-1-4.4-15.

Duvigneau, R., Visonneau, M. and Deng, G.B. (2003), “On the Role Played by Turbulence Closures in Hull Ship Optimization at Model and Full Scale”, Journal of Marine Science and Technology, 8, 11-25.

Felli, M., Camusi, R. and Di Felice, F. (2011), “Mechanisms of Evolution of the Propeller Wake in the Transition and Far Fields”, Journal of Fluid Mechanics, 682, 5-53.

Guilmineau, E., Deng, G.B. and Wackers, J. (2011), “Numerical Simulation with DES Approach for Automotive Flows”, Journal of Fluids and Structures, 27, 807-816.

Leroyer, A. and Visonneau, M. (2005), “Numerical Methods for RANSE Simulations of a Self-Propelled Fish-like Body”, Journal of Fluids and Structures, 20, 975-991.

Muscari, R., Di Mascio, A. and Verzicco, R. (2013), “Modeling of Vortex Dynamics in the Wake of a Marine Propeller”, Computers and Fluids, 73, 69-79.

Queutey, P. and Visonneau, M. (2007), “An Interface Capturing Method for Free-Surface Hydrodynamic Flows”, Computers and Fluids, 36, 1481-1510.

Wackers, J., Deng, G.B., Guilmineau, E., Leroyer, A. Queutey, P. and Visonneau M. (2014), “Combined Refinement Criteria for Anisotropic Grid Refinement in Free-Surface Flow Simulations”, Computers and Fluids, 92, 209-222.

DISCUSSION

Question from Douwe Rijjpkema

Did you already investigate the pressure inside the core of the vortex? This is of good interest when calculating cavitation.

Authors' Closure

Thank you for your question and your suggestion. Since we also consider the cavitation risk, the evolution of pressure was investigated. The evolution of pressure for J = 0.71 in the plane Y = 0 mm for is presented in Figure I. The most significant modeling effect is a high dissipation of the intensity of vortices, and of minimum pressure levels, with RANS models. With DES, the lowest pressure level is maintained further downstream. This is what we expect from the physics. However, if this trend is encouraging, it remains to validate a DES simulation including the cavitation modelling.

Question from Antoine Ducoin

You use two turbulence RANS models that predict different level of turbulent kinetic energy in the wake/tip vortex. Is it an important parameter to avoid the diffusion of the vortex in the wake? If no, how do you analyze the differences on the λ_2 plots?

Authors' Closure

Thank you for your question. For both RANS models, there is no parameter to avoid the diffusion of the vortex in the wake. Both RANS models predict an increase of the turbulence kinetic energy in the wake that destroys the tip vortex. With the DES approach, the prediction of the turbulent kinetic energy in the wake is lower than that predicted with the RANS models.

Question from Tobias Huuva

How did you model the rotation of the propeller in the computation? How will you do when including the rudder? How much longer time step for DES? For RANS?

Authors' Closure

Thank for you question. The equations are written in the moving reference frame but written in terms of absolute reference quantities. When a rudder will be present, two solutions are available. The first is the use of the sliding grid. It depends on the position of the rudder with regard to the propeller and the hull. The second option is the use of overset. The number of time steps for DES is approximately 16,200 and the CPU time per processor is 300 hours. For RANS, the number of time step is approximately 4,000 time steps and the CPU time per processor is 23 hours. All simulations are distributed on 96 processors.

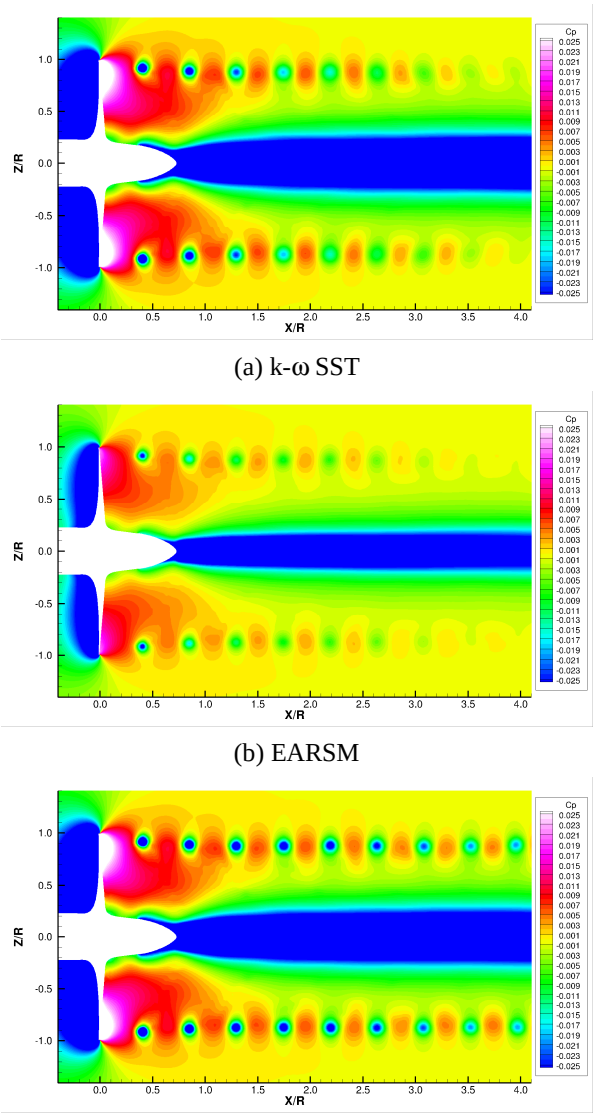

(a) k-ω SST

(b) EARSM

(c) DES

Figure I: J = 0.71 - Pressure coefficient in the plane Y = 0.